Monosodium glutamate (MSG) perturbs trophoblast differentiation and invasion program through a ROS-mediated pathway

Indrani Mukherjee
Amity University
Sunil Singh
All India Institute of Medical Sciences
Subhrajit Biswas
Amity University
Joyeeta Talukdar
All India Institute of Medical Sciences
Mohammed S. Alqahtani
King Khalid University
Mohamed Abbas
King Khalid University
Tapas Chandra Nag
All India Institute of Medical Sciences
Asit Mridha
All India Institute of Medical Sciences
Surabhi Gupta
All India Institute of Medical Sciences
Jai Bhagwan Sharma
All India Institute of Medical Sciences
Supriya Kumari
All India Institute of Medical Sciences
Ruby Dhar
All India Institute of Medical Sciences
Subhradip Karmakar (subhradip.k@aiims.edu)
All India Institute of Medical Sciences

Article

Keywords: Trophoblast, Monosodium glutamate, Preeclampsia (PE), Reactive oxygen species (ROS), Oxidative stress (OS), Trophoblast dysfunction

Posted Date: August 29th, 2022

DOI: https://doi.org/10.21203/rs.3.rs-1867105/v2

Abstract

Monosodium glutamate (MSG) is a flavor-enhancing food additive widely used in Asian cuisine. It is one of the common ingredients used in curry and other tinned food that is believed to bring out the "umami" meat flavor and enhance the savory taste of the food. It is the sodium salt of the naturally occurring amino acid Glutamate. Due to its massive consumption as part of fast-food culture along with concerns about its possible effect on health in general and pregnancy in particular, we undertook this study to address its impact on placental trophoblast cells. We investigated the effect of MSG on placental trophoblast cells. Our studies confirmed that short and long-term exposure to MSG has a profound influence on trophoblast invasion and differentiation, two of the most critical and dispensable functions during placentation. Our results showed an acute short-term MSG-treatment enhanced trophoblast invasion and cell motility along with an increased expression in trophoblast cell differentiation markers. However, long-term chronic MSG stimulation in these cell types showed the opposite effect with both reduced invasion and differentiation. Further, MSG-treated placental explants displayed signs of elevated oxidative stress. These effect of MSG on trophoblast cells along with an increased ROS production indicates that long-term usage of MSG as part of food additive might have adverse health consequences on the developing embryo by compromising the trophoblast and placental function.

1. Introduction

The global glutamic acid market size was estimated at over 2.9 million tons in 2014 and is likewise more than 4 million tons by 2023[1]. The MSG-related revenue is expected to be worth more than USD 15.5 billion by 2023, growing with an estimated CAGR(Compound Annual Growth Rate) of above 7.5% up to 2023[1]. China is the largest consumer of these products. China alone accounted for more than 52% of global MSG consumption[2,3]. With such an enormous appetite for this additive in the food industry, the health concerns are also substantial, given that MSG administration is reported to increase the number of pachytene stage cells in the primary spermatocytes[4,5] and induce oxidative stress[6,7] and free radical generation[8,9]. In addition, obesity[10–13], CNS disorder[14–16], hepatic damage[17–19], reproductive malfunctions[4,20–22], cardiovascular[23,24], and hypertension[25–27] are considered to be some of the major side effects of MSG consumption.

Despite these observations, detailed molecular pathogenesis related to MSG consumption is poorly understood. In this present study, we want to investigate the effect of MSG on placental trophoblast cells and extrapolate its possible consequences on pregnancy outcomes. This is essentially due to the prime importance of the placenta in sustaining a pregnancy and supporting fetal growth and development. Trophoblast cells constitute the functional and structural component of the placenta's supporting the pregnancy by orchestrating delicate feto-maternal cross-talk and its endocrine function. This also involves the exchange of nutrients and waste across the feto-placental unit. Trophoblast cells are pseudo-malignant[28] and transiently invasive[29], participating in remodeling the maternal uterine matrix and its vasculature to gain access to its nutrient-rich milieu. Successful pregnancy depends on how efficiently this process is accomplished. Much of this in turn depends on an efficient trophoblast differentiation program. MSG exposure seems to perturb this delicate process. Our findings reveal an oxidative stress response originating upon MSG exposure to the trophoblast cells affecting its invasion and differentiation.

2. Results

2.1 Effect of monosodium glutamate stimulation on trophoblast cell viability and cell proliferation

The sub-lethal dose of monosodium glutamate and its toxic effects on trophoblast cell lines were evaluated using the water-soluble tetrazolium-1 (WST-1) Assay. Compared to the untreated controls, MSG significantly decreased cell viability in a dose-dependent manner in the HTR8/SV neo (Fig, 1A) and BeWo cells (Fig, 1B). Results obtained using Trypan Blue staining were in agreement with the WST-1 assay in both the cell lines (Fig, 1C, and D). Annexin-V/PI staining was also done in both the cell lines to check cell death, and data showed that more than 75% of cells were viable when treated with 25 mM and 50 mM MSG for acute stimulation and 25 mM for chronic stimulation in both HTR8/SV neo and BeWo cells. (Suppl. Fig, 2A-D) We also performed cell cycle analysis after acute stimulation of MSG for 24 h, and the results showed that there was a nonsignificant change in the G1, S phase of BeWo after stimulating the cells with both 25 mM and 50 mM MSG as compared to the untreated control group. However, there was a significant increase in the percentage of cell proliferation of the G2 phase in 50 mM MSG stimulated BeWo cells (Suppl. Fig, 2E), but no significant change was observed in the percentage of S phase cells in HTR8/SV neo cells compared to control untreated cells. (Suppl. Fig, 2F) Similarly, in the chronic stimulation groups, cell cycle analysis was done to assess the percentage of cell proliferation, and data showed that there was no significant difference in cell proliferation between the Control and the treated groups in both BeWo cell lines. (Suppl. Fig, 2G-J) and HTR-8/SV neo (Suppl. Fig, 2K-N). Therefore, 25 mM MSG & 50 mM both were used for studying the acute effects of MSG, and 25 mM MSG was used to study the effects of its chronic stimulation in the trophoblast cell lines in the subsequent experiments.

2.2 Acute stimulation of monosodium glutamate increases differentiation and invasion in trophoblast cells and early placental explants

To assess the effect of monosodium glutamate (MSG) on trophoblast differentiation, BeWo cells were analyzed for the expression of well-established trophoblast differentiation markers like Syncytin-1 (SYN-1), Syncytin-2 (SYN-2), and Glial Cells Missing-1 (GCM1). Dysferlin (DYSF) and β subunit of human chorionic gonadotropin (β-hCG), were also used. Results showed that both doses of MSG (25 mM and 50 mM) significantly increased the expression of SYN-1, SYN-2, DYSF, GCM-1, and β-hCG in mRNA levels (Fig, 2A-E). The concentration of β-hCG was also evaluated in the conditioned media of the cells and results showed significant upregulation of β-hCG in the protein level after acute stimulation of both the doses of MSG (25 mM and 50 mM) (Fig, 2F). We next evaluated the effect of MSG in the early placental explants derived from FT chorionic villi obtained from MTP cases (8-12 weeks of pregnancy). Results showed that the expression of SYN-1, SYN-2, DYSF, GCM1, and β-hCG were significantly upregulated ($P<0.01$). Gene expression of the receptors of Syncytin-1 and Syncytin-2, i.e, Solute Carrier Family 1 Member 5 (SLC1A5) and Major Facilitator Superfamily Domain Containing 2A (MFSD2A) respectively also showed similar trends. (Fig, 2G) . β-hCG protein levels were significantly upregulated in the early explants treated with 50 mM MSG. (Fig, 2H). Taken together, MSG upregulated trophoblast differentiation markers in the trophoblast cells and tissue explants significantly.

We next interrogated the effects of MSG on trophoblast invasion. Using the EVT-derived early trimester trophoblast cells HTR-8/SVNeo, we assessed the mRNA expression of invasion-associated genes MMP-2, MMP-9 & uPA and their inhibitors TIMP-1, TIMP-2 & PAI-1. Results showed significant upregulation of all the proteases in both doses of MSG as compared to the untreated controls($p<0.05$). (Fig, 3A, B, and E). MSG treatment (50 mM) showed a significant decrease in the TIMP-2 and PAI without alterations in TIMP-1 expression (Fig, 3C, D, and F). Interestingly, we also observed an elevated expression of ONZIN/PLAC8 (Placenta associated 8), with both doses of MSG ($p<0.01$). ONZIN was earlier reported[30] to be positively associated with the invasiveness and migratory behavior of trophoblast cells (Fig, 3G). Results from western blot in the HTR-8/SV Neo cells showed similar trends, with MSG stimulation showing an increased expression of the trophoblast proteases (MMPs) along with reduced expression of the protease inhibitors(TIMPs). TIMP-1 expression showed a reduction only at 50 mM MSG (Fig, 3H-L)

To further confirm that the pro-invasive effect of MSG on HTR-8/SV cells as seen in the invasion assay is due to the secretion of MMPs, a functional assay was performed using gelatin zymography. Results of zymography showed significant upregulation of gelatinolytic MMP-2 and MMP-9 bands in both 25 mM, and 50 mM MSG-stimulated HTR-8/SV neo cells. (Fig, 3M-O). Matrigel invasion assay showed a similar trend with significant upregulation of the average number of the invaded cells per field in the HTR-8/SV neo cells after acute stimulation of MSG. (Fig, 3P, and Q) Wound-healing assay performed with HTR-8/SV neo cells showed that the MSG-treated cells (both doses) had a significantly higher migration rate compared to control untreated cells. ($p<0.01$) (Fig, 3R, and S). To further elucidate the effect of short-term MSG exposure on the invasive potential of the early placental explants, we assessed the gene expression for invasion markers. Results showed (Fig, 3T) that the proteases MMP-2, MMP-9, and uPA were significantly upregulated in the explants; however, TIMPs (1&2) were significantly downregulated. PLAC8 mRNA expression was also found to be significantly higher in the MSG-treated group. Therefore, acute stimulation of MSG is responsible for the increased differentiation and invasion in the trophoblast cells as well as in the early placental explants.

2.3 Long-term chronic stimulation of Monosodium glutamate decreases differentiation and invasion in trophoblasts

Consistent with the findings so far, we assessed the mRNA expression of the previously chosen genes responsible for differentiation of the trophoblast cells in case of chronic stimulation (16 days) of 25 mM MSG after Day 4, Day 8, Day 12, and Day 16 of stimulation by treating the BeWo cells every alternate day for the entire span of 16 days. Surprisingly, we observed an opposite trend with a significant decrease in SYN-1, SYN-2, SLC1A5, MFSD2A, DYSF, GCM1, and β-hCG on all four days of collection ($p<0.01$). (Fig, 4A-G) We also assessed the protein expression of β-hCG on all four days, which showed a significant reduction trend on all four days. (Fig, 4H)

In order to determine the effect of chronic stimulation of MSG on the invasion of the trophoblast cells, we analyzed the gene expression of the previously studied genes in case of acute stimulation. Interestingly, we observed that the proteases MMP-2, MMP-9, and uPA were significantly downregulated on Day 4, Day 12, and Day 16. While MMP-9 was ~3fold downregulation, MMP-2 and uPA also showed downregulation, though not that significant on Day 8 (Fig, 5A, B, and E). mRNA expression of TIMP-1 and TIMP-2 was upregulated on all four days of collection, we observed that the fold change in TIMP-1 on days 8 & 12 and TIMP-2 on Day 4 was not that significant. (Fig, 5C, and D) PAI, on the contrary, though was slightly upregulated on Day 4 and Day 8, was eventually downregulated on Day 12 and Day 16 of stimulation; (Fig, 5F) PLAC8 was also significantly downregulated on Day 4, 12, and 16;. (Fig, 5G)

Western blot was performed to confirm the RT-PCR findings. Protein expression of MMP-1,2 and TIMP-1,2 showed that MMP-2 was significantly downregulated on all four days of collection, while TIMP-2 was upregulated on Day 4, Day 8, and Day 16. (Fig, 5H, J, and L) . MMP-9 and TIMP-1 were significantly upregulated on Day 4 and Day 16 whereas, on Day 8, we observed downregulation in the protein expression of both MMP-9 and TIMP-1. We also observed that Day 12 showed an opposite trend for both MMP-1 and TIMP-1, where MMP-9 was downregulated, and TIMP-1 was significantly upregulated. (Fig, 5I, K)

Consistent with our previous findings, gelatin zymography revealed that the activity of both MMP-2 and MMP-9 was significantly reduced in the HTR-8/SV neo cells after chronic stimulation of MSG on all four days of collection. ($p<0.05$) (Fig, 5M, N, and O). Matrigel invasion assay and wound healing assay performed after 16 days of chronic MSG stimulation, showed less number of invading cells along with reduced migration (Fig, 5P-S) . Therefore all the above findings indicate that chronic stimulation of MSG significantly downregulates the invasive and migratory properties of the trophoblast cells.

2.4 Stimulation of MSG induces oxidative stress in the cells and tissues

MSG is reported earlier to elicit oxidative stress[31,32]. In order to explore a similar mechanism in the trophoblast cells (HTR-8/SV neo and BeWo), we measured the concentration of Thiobarbituric Acid Reactive Substances (TBARS) in both the groups of our study, i.e., acute and chronic stimulation of MSG. Results showed that there was significant upregulation of TBARS in cells treated with 25 mM MSG and 50 mM MSG for 24h. To check the specificity of the observation, we performed rescue experiments with N-Acetyl cysteine (NAC) Interestingly, NAC could significantly downregulate the concentration of TBARS in the trophoblast cells *in vitro* for both26 the chosen doses. ($p<0.01$) thereby implying a ROS-mediated process.(Fig, 6A, and B) .

A similar study performed on the chronic MSG stimulation group revealed a significant upregulation in TBARS concentration on all four days of the collection. However, in the HTR-8/SV neo cells, NAC failed to quench the reactive oxygen species produced in the cells on Day 16, while in BeWo cells, there was a significant decrease of TBARS in the group pretreated with NAC on days 4,8,12, and 16 after stimulating the cells with 25 mM MSG on every alternate day. (Fig, 6C, and D) Similarly, we measured the concentration of TBARS in the early placental explants, and data revealed that there was an increase in the TBARS concentration in the treatment group compared to the control group. (Fig, 6E) To further reconfirm the induction of oxidative stress in the trophoblast cell lines, we stained the cells with CellRox and showed a right peak shift in the cells treated with MSG in both acute and chronic conditions as compared to the untreated control group. However, cells pretreated with NAC showed low levels of ROS, similar to the control group. The mean fluorescence intensity was measured, and the cells pre-stimulated with MSG and NAC had no change in peak shift compared to the MSG-only group suggesting that NAC prevented the generation of ROS in the cells. (Fig, 6F-I) Similarly, we confirmed the induction of oxidative stress due to chronic stimulation of MSG in the early placental explants by performing an immunohistochemical analysis. Results showed that the expression of NRF2 was significantly downregulated in the group where

the explant tissues were treated with 50 mM MSG for 72 h. (Fig, 6 J) Western blotting was performed in both the trophoblast cell lines to confirm the generation of reactive oxygen species in the cells, and the expression of NRF2 was assessed in the cell lysates of BeWo and HTR-8/SV neo cell lines. Densitometric analysis was done in both the trophoblast cell lines. Data showed that the expression of NRF2 was significantly downregulated in both the cell lines treated with 25 mM MSG for 24h. (Suppl. Fig, 3A-D) Taken together, MSG induced oxidative stress in both the trophoblast cell lines as well in the early placental explant.

2.5 Ultrastructural features alter in early placental explants as a result of chronic stimulation of MSG

Further, we investigated the cause of the altered trophoblast function in the placental tissue explants with speculation of a ROS-mediated intracellular injury post-MSG stimulation. Using Transmission Electron Microscopy (TEM), we explored the ultrastructural details of the early placental tissue explants after a chronic stimulation of 50 mM MSG for 72h. Significant ultrastructural changes were observed in the placental explant tissues (n=10) compared with the control explant tissues. Disintegrated syncytiotrophoblasts (Fig, 7A), short and distorted microvilli (Fig,7B), high glycogen content (Fig,7C), and totally disintegrated nucleus (Fig, 7D) were observed in tissue explants treated with MSG compared to the healthy untreated control explants. Interestingly, we observed disintegrated mitochondria (Fig,7E) and swollen ER (Fig, 7F) in the MSG-treated tissue explants. All the above results indicate the fact that MSG causes ultrastructural changes in the placental explant tissues.

2.6 Induction of oxidative stress by MSG in the cells causes the induction of ER stress in the trophoblast cells

TEM data indicated that MSG altered the ultrastructure of mitochondria and endoplasmic reticulum in the early villi explants treated with 50 mM MSG. In accordance with this, and to explore the underlying mechanism, we checked the expression of the proteins involved in the unfolded protein response pathway in the BeWo and HTR-8/SV neo cell lines treated with 25mM and 50 mM MSG for 24h. Immunoblotting data showed that there was significant upregulation of BiP in the BeWo cells after 50 mM MSG stimulation Fig. 8 (A, B), whereas 25 mM MSG did not have any significant change in the protein expression of BiP. However, we observed that in HTR-SV neo cells, there was a significant upregulation of BiP in the 25 mM MSG treated group compared to the 50 mM MSG treated cells Fig, 8 (F, G). In BeWo cells, there was a significant upregulation of phosphorylated IRE1a (pIRE1a) in the groups treated with 25mM MSG and 50 mM MSG after 24h of stimulation Fig, 8 (A, C), whereas, in the HTR-8/SV neo cell, there was a significant upregulation of pIRE1a in the group stimulated with 50 mM MSG Fig, 8 (F, H). The expression of IRE1a was significantly upregulated in the 50 mM MSG group in the BeWo cells Fig. 8 (A, D), and we observed quite the opposite in HTR-8/SV neo, where there was significant upregulation of IRE1a in the 25 mM MSG stimulated group Fig, 8 (F, I). Xbp1 was significantly upregulated in the 25 mM MSG stimulated group in the BeWo cells Fig, 8 (A, E), whereas there was significant upregulation of Xbp1 in the 50 mM MSG stimulated group in the HTR-8/ SV neo cells observed after 24h of stimulation Fig, 8 (F, J). We also checked the expression of Xbp1 in the early placental explant tissues, and the results of immunohistochemistry showed that there was a significant upregulation of Xbp1 in the MSG-treated group compared to the untreated early villi explant group (Fig, 6J g,h). All these results showed that MSG caused OS-induced ER stress in placental trophoblast cells.

3. Discussion

MSG is a widely used food additive consumed as part of several culinary dishes worldwide. It is one of the majorly used food additives[33–35] used rampantly worldwide. Though MSG is also found naturally in foods, like tomatoes, we see its maximal usage as an external additive and flavor enhancer. MSG consumption in experimental animals predisposes to obesity, insulin resistance, reduced glucose tolerance, and metabolic disorders causing disrupted energy balance[13,36–39]

Further, Roman-Ramos et al.[40] reported an elevated interleukin-6 (IL-6), tumor necrosis factor-alpha (TNF-α) mediated inflammatory response upon MSG exposure through a micro-RNA (mRNA) pathway. Apart from its metabolic effect, MSG in both rodents and human has a detrimental effect on the reproductive system, involving an increased number of pachytene stage cells among the primary spermatocytes[5,41], MSG exposure in mice also causes disruption of the basement membrane of the theca follicle in the ovary leading to atrophy and degeneration[4,5,42]. This seems to be due to enhanced oxidative stress leading to DNA and chromatin damage, and adduct formation, in the stromal cells[9,43].

Despite such a clear indication of the harmful effects of MSG on human physiology[44], there is hardly any conclusive study performed to investigate its short and long-term effect on placentation or on pregnancy outcome. A quick literature search in Pubmed with the keywords "MSG and human placenta /trophoblast" yielded no significant studies, thereby suggesting that not much is investigated in this direction.

The global market for Monosodium Glutamate (MSG) is estimated at US$3.8 Billion in 2020 and is projected to attain a revised size of US$4.7 Billion by 2027[45]. The MSG market in the U.S. alone is estimated at $1 Billion in the year 2020. Presently, the world's largest MSG consumer and producer is mainland China[46]. With such an enormous consumption worldwide[47] with the possibility of its harmful effect on humans, we undertook this study to address the effect of MSG on trophoblast function and to explore the underlying molecular mechanisms. Our study identified critical pathways related to trophoblast invasion and differentiation that are perturbed upon MSG exposure using cell line-based models and placental explants. Further MSG elicited an ER stress response mediated through the BiP and IRE1a pathways in HTR-8/SVNeo as well as BeWo cells. MGS also induced oxidative stress, as evidenced by an elevated ROS production. This resonates with previous reports of MSG-inducing OS[24,48,49]. Our study also found MSG exposure (24 hrs) increases trophoblast cell migration and invasion while an extended exposure (14 days) reduced both. We thus see a dual effect of MSG in this aspect. This brings to us an interesting question that why does MSG show this dual response? Based on the previous reports[50], we hypothesize, that low levels of ROS(upon short-term MSG treatment) could enhance trophoblast invasion by multiple mechanisms like the formation of invadopodia[51] , engaging SRC family of kinases, c-Jun N-terminal kinase (JNK) and p38 kinase[52] ; ROS may also activate PKC through the release of intercellular calcium stores[53] enhancing cell proliferation. According to the “two-wave theory of invasion”[54] an initial event of shallow trophoblast invasion within the decidual layer is followed by a pause until around week 12 of gestation (in

humans), leading to the second wave of a more extended interstitial and endovascular invasion[54] that results in rapid maternal blood flow in the intervillous space establishing hemochorial placenta[55]. The intervillous space is actually oxygen deficit before week 12 of human gestation. This creates transient hypoxia which in turn is imperative for initiating trophoblast invasion and placental angiogenesis by HIF-mediated activation of VEGF[56,57]. We, therefore expect to witness a step-by-step well-regulated increment in oxygen in the feto-maternal space[58,59] that should parallel with a step-by-step increase in the trophoblast invasiveness so as to maintain the adequate oxygen gradient. The importance lies in the synchrony of this entire process. A premature trophoblast invasion is as detrimental as an inadequate trophoblast invasion, with both resulting in serious consequences[60]. One way to safeguard this premature trophoblast invasion is trophoblast-mediated sealing of uterine arteries forming plugs that prevent rapid blood flow and oxygenation at the feto-maternal interface[61].

As a matter of fact, MSG treatment (short exposure: 24 hours) in our study enhanced migration and invasion of the extravillous trophoblast cells HTR-SVNeo. We, therefore, speculate that MSG could potentially offset the fine balance necessary to establish the physiological oxygen gradient by perturbing the invasion. Since MSG in our study also generated ROS, it could involve a ROS-dependent process. Our long-term MSG treatment however downregulates both invasion and differentiation. This could be accounted as a consequence of an excess of ROS production that seems to exhaust the cellular antioxidant defense systems (as seen by downregulation of Nrf2) leading to loss of invasion potential of these cells[62] or could further lead to their apoptosis[63,64].

Trophoblast invasion is a highly coordinated process that involves the remodeling of maternal vasculature and invasion of the endometrium. The success of this process heavily depends upon the orchestrated effort of pro and anti-invasive proteins in a tempo-spatial manner[65,66]. MSG tilts this delicate balance, thereby perturbing the trophoblast invasion and differentiation program. MSG also enhanced the production of ROS, leading to cellular damage, as evident from the biochemical and ultrastructural studies. MSG treatment depletes the antioxidant Nrf2, as found in the placental histology. Nrf2 in turn regulates the antioxidant defense system through multiple mechanisms[67–69]. Loss of Nrf2 upon MSG treatment, therefore, induces oxidative stress. A previous study from our lab[70] identified ROS-mediated activation of UPR pathways which in turn leads to altered trophoblast function. The present study establishes the link that MSG is possibly operating through a similar mechanism. These findings indicate that long-term consequences of MSG consumption on placenta trophoblast cells might have an adverse effect on the conceptus though we don't have experimental evidence at this point to support our statement. Our study is preliminary in this direction. Further efforts are undertaken using rodent models to delineate the *in-vivo* effect of MSG on pregnancy outcomes.

4. Materials And Methods

4.1 Cell Culture

HTR-8/SV neo cells and BeWo (choriocarcinoma cells) were obtained from American Type Culture Collection (ATCC, Rockville, MD, USA). Cells from relatively early passages (R=3) were cultured using RPMI-1640 medium (HyClone) containing 1% penicillin-streptomycin (Invitrogen) and 10% FBS (Invitrogen)[70].

The cells were plated on a 90 mm petri dish at a concentration of 1 x 10^6 cells/petri dish and cultured at 37°C in a humidified chamber with 5% CO2. The experiments were broadly divided into two categories based on the type of stimulation- Acute Stimulation and Chronic Stimulation. Acute stimulation groups were divided into three sub-groups - (i) control, (ii) cells treated with 25 mM monosodium glutamate (MSG) for 24 h, (iii) cells treated with 50 mM monosodium glutamate (MSG) for 24 h. (Suppl. Fig, 1A and B) Chronic stimulation groups were divided into two sub-groups - (i) control, (ii) cells treated with 25 mM Monosodium glutamate (MSG) every alternate day for 16 days. (Suppl. Fig, 1C and D) Cells were then scraped and processed for RNA and protein extraction.

To confirm the presence of oxidative stress in the acute conditions, cells were divided into two more sub-groups- (iv) cells treated with 10 mM N-acetyl cysteine (NAC), a potent antioxidant, for 24 h, and (v) cells pretreated with NAC for 2 h followed by MSG treatment for another 24 h. To perform rescue experiments in the chronic conditions, cells were divided into two more sub-groups, (a) cells treated with 10 mM N-acetyl cysteine (NAC), a potent antioxidant on every alternate day, and (b) cells pretreated with NAC for 2 h followed by MSG treatment on every alternate day. At 50-60% confluence, cells were kept in a phenol red-free medium containing 5 % FBS and treated with NAC and the two sub-lethal doses of MSG.

4.2 Explant culture

First-trimester placental samples of different gestational ages between 8-10 weeks were obtained from medically terminated pregnancies (n=10) after delivery, and their tissue explants were cultured. The Institutional Human Ethics Committee at the All India Institute of Medical Sciences, New Delhi, India, approved the study protocol (IEC-225/05.04.2019) and all methods were performed in accordance with the relevant guidelines and regulations. All participating subjects gave their written consent and Informed Consent was obtained from the participants in the study

Small sections, each weighing 10 mg, were cut and plated in Collagen-I coated single well of 12 well plates (Corning). The tissue sections were washed thoroughly using 1X phosphate-buffered saline (PBS) followed by the addition of RPMI-1640 medium (HyClone) having 10% FBS (Invitrogen) and 1% penicillin-streptomycin (Invitrogen). The culture plate was then cultured at 37°C in a humidified chamber with 5% CO2[70] . For experimental purposes, sections from each early villi were divided into two groups- (i) control and (ii) sections treated with 50 mM MSG for 24 h. (Suppl. Fig, 1E) Tissues were then collected in the TriZol (Thermo Fisher Scientific) and processed for RNA isolation. The explants were also divided into two more sub-groups- (i) explants treated with 10 mM N-acetyl cysteine (NAC) for 24 h, and (ii) explants pretreated with NAC for 2 h followed by MSG treatment for another 24 h to perform the oxidative stress experiments where NAC was used in combating the MSG mediated reactive oxygen species (ROS) generation in the explants. The explants were also stimulated for 72h to study the ultrastructural changes in the tissue explants after chronic stimulation of MSG.

4.3 RNA isolation and reverse transcription-quantitative polymerase chain reaction (RT-qPCR)

Total RNA was extracted from the cells using the RNA Simple Total RNA isolation kit (Promega RNA Tissue/Cell Miniprep System)according to the manufacturer's instructions. An in-column DNAse digestion was performed to obtain DNAse-free RNA. RNA was quantified using Nanodrop (Thermo Fisher Scientific, Inc.), followed by an agarose gel electrophoresis to check the integrity of the. It was then reverse transcribed into cDNA using the Verso cDNA synthesis kit (AB1453A, Thermo Fisher Scientific, Inc.). RT-qPCR was performed using DyNAmo Flash SYBR Green qPCR kit (F415S, Thermo Fisher Scientific, Inc.). The qPCR reaction cycles were as follows: incubation at 95ºC for 7 mins, 40 cycles at 95ºC for 15 sec, and 60ºC for 20 sec(Applied Biosciences). The PCR products were subjected to a melting curve analysis to confirm the amplification specificity. mRNA levels were then normalized with respect to the housekeeping GAPDH mRNA levels using the 2-ΔΔCq method[70]. PCR primer sequences have been provided in the Suppl. Table 1.

4.4 Cell viability and proliferation assay

Cells were plated in 96 well plates. Cells were then treated with different doses of MSG. Water-soluble tetrazolium- 1 (WST-1) assay was performed to check the proliferation and viability of the cells following the usual manufacturer's protocol. Results were analyzed after comparing to a standard curve[70].

4.5 Cell cycle and apoptosis assay

For cell cycle assay, log phase MSG treated trophoblast cells (HTR-8/SV neo and BeWo) were collected, washed with 1X PBS, and fixed with 70% ethanol overnight at 4˚C. After washing twice with 1X PBS, the cells were resuspended and incubated in 500 µl PBS containing 100 µg/ml RNase and 50 µg/ml propidium iodide (PI) solution for 30 min at room temperature. Cells were acquired by flow cytometry(ThermoFisher Scientific, Cat No. V13242), and the percentage of cell proliferation was analyzed using GraphPad PRISM version 6.01.

Apoptosis assays were performed by flow cytometry using Annexin V-FITC/propidium iodide double-label assay, according to the manufacturer's protocol (BMS500FI/100CE, Invitrogen). The treated cells (1×10^6) were trypsinized and incubated in 100 µL binding buffer containing 5 µL AnnexinV/FITC and 10 µL 20 µg/mL P.I. for 15 mins in the dark at room temperature. 10,000 events/runs were acquired, and the results were analyzed using FlowJo software (Ashland, OR, USA)[70].

4.6 ROS production

Cells were plated in 12-well plates. Post MSG treatment, as mentioned above, 5 µM CellRox (Cellular ROS Assay Kit, ab186029S) was added to each well and was kept for incubation for 30 mins at 37 °C. The cells were then washed three times with 1X PBS at room temperature and analyzed by flow cytometry using BD FACSCantoTM[70].

TBARS Assay

Thiobarbituric Acid Reaction Species Assay (Cayman Chemicals) was performed to estimate the Malondialdehyde (MDA) levels, the final product of lipid peroxidation. Thiobarbituric acid reactive substances (TBARS) concentrations were measured at 532 nm in cells according to the manufacturer's protocol.

4.7 Western Blotting

Cell lysates were prepared using 1XRIPA buffer, containing protease and phosphatase inhibitors. 60ug of lysates were electrophoresed in 10% discontinuous SDS-PAGE for western blotting (W.B.) Gels were transferred to the polyvinylidene difluoride (PVDF) membrane. After the transfer, nonspecific binding to the membrane was blocked in 5% non-fat milk for 1 hour. These were then incubated with primary antibodies overnight at 4°C followings which the membrane was washed in TBST and then incubated with Horseradish Peroxidase (HRP)-conjugated 2° antibody at room temperature for 1 hour. Bands were visualized using the enhanced chemiluminescence (ECL) (NCI4106; Thermo Fisher Scientific, Inc.)[70] . The same membranes were used for reprobing with an antibody against GAPDH (Cell Signalling Technology, Beverly, MA) (1:1500). Semi-quantitative estimation of band intensities was performed using Image J.

Antibodies used:

Rabbit polyclonal anti-MMP-2, rabbit polyclonal anti-MMP-9, rabbit polyclonal anti-TIMP-1, and rabbit polyclonal anti-TIMP-2, all from Cell Signal Technology, Beverly, MA, and rabbit polyclonal anti-BiP, rabbit polyclonal anti-XBP1, rabbit polyclonal anti-pIRE1, rabbit polyclonal anti-IRE1, rabbit polyclonal anti- NRF2, all from ABclonal Technology, Cumming Park were used at 1:1000 dilution in 5% BSA solution containing 0.1% TBST and kept at 4 ºC overnight. Enhanced chemiluminescence (ECL) (NCI4106; Thermo Fisher Scientific, Inc.) was used to detect proteins. Finally, a densitometer was used to quantify the immunoreactive signals. The same membranes were used for reprobing with an antibody against glyceraldehyde-3-phosphate dehydrogenase (GAPDH) (Cell Signalling Technology, Beverly, MA) at 1:1500 dilution.

4.8 Gelatin Zymography

Bioactivity of secreted matrix metalloproteinase (MMP)–2/9 in the conditioned media of HTR-8/SVneo cells was measured using substrate gel gelatin zymography. 8% polyacrylamide gel containing 0.1% gelatin was used to resolve proteins. 2.5% Triton X-100 solution was used to wash the gels for 1 h to renature the proteins, followed by washing with distilled water and incubation in activation buffer (150mM NaCl, 10mM CaCl2, 50mM Tris, and 0.025% sodium azide) at 37 degrees with gentle shaking overnight. 0.1% Coomassie brilliant blue was used to stain the gels for 30 mins, followed by de-staining with 10% acetic acid solution to visualize[70].

4.9 Wound Healing Assay/Cell Migration assay

Cells were seeded in 6 well plates at a density of 2×10^5 cells per well until they reached 80-90% confluence. A small pipette tip was used to make a scratch through the cell monolayers, and the debris was removed using 1X PBS. Cells were treated as previously mentioned. After treating the cells for 24h, images were captured at regular intervals until complete wound healing (filling up of the scratch with cells) using a phase-contrast microscope[70].

4.10 Matrigel Invasion Assay

The invasion assay was performed using a 24-well insert system (8 µm pores; Transwell chamber, Millipore). The insert plate surface was coated with 50 µl of diluted matrigel (356234; Becton Dickinson and Company, Franklin Lakes, New Jersey, USA, 1:9 in RPMI-1640). 200 uL of HTR8/SV neo cell suspension (1.0 × 105 cells) was seeded into the insert, and FBS supplemented culture medium was added to the reservoir well. After that, the cells were treated and cultured for 24 h. A swab was used to remove the remaining trophoblast cells from the upper insert after incubation. The trophoblast cells which infiltrated and reached the other side of the insert were fixed with ice-cold methanol and stained with 4',6-Diamidine-2'-phenylindole dihydrochloride (D9564, Sigma-Aldrich) for nuclear staining and Alexa Fluor® 488 Phalloidin (green) (Cell Signalling Technology, Beverly, MA) for cytoplasmic staining. Images obtained were captured using an upright microscope (TI-E, 601869, Nikon Laser Scanning Confocal Microscope) at 200X magnification[70].

4.11 Transmission electron microscopy

Early Placental explant tissues (1 mm3/piece) or cell pellets (10^6) treated with 50mM MSG for 72h were fixed with Karnovsky's fixative at 4°C, rinsed with 0.1 M phosphate buffer (pH~7.4) twice, and post-fixed with 1% osmium tetroxide for 1 h. Samples were then dehydrated in acetone, embedded in Araldite CY212, and polymerized. Sections (60–70 nm thick) were cut and stained with uranyl acetate and lead citrate. Sections were examined using a Talos 200S transmission electron microscope (Thermo Scientific, Inc.) at the All India Institute of Medical Sciences, New Delhi, India[70]

4.12 Immunohistochemistry

Early placental explant tissue samples treated with 50mM MSG for 72h were washed in PBS and fixed overnight in 4% buffered formalin at 4 degrees. Samples were then washed to remove the fixative and paraffin-embedded 5 µm thick sections were cut in microtome (ThermoFisher Scientific, Cat no 36000). The sections were deparaffinized, rehydrated, and microwaved for 20 minutes in Tris-EDTA buffer (pH 9.0) for antigen retrieval. Endogenous peroxidase was quenched with 3% H_2O_2 for 15 min. Non-specific binding was blocked using BlockAid™ Blocking Solution (Invitrogen). Sections were incubated with rabbit anti-NRF2 antibody (dilution: 1:1000; ab137550; Abcam) and rabbit anti-Xbp1s antibody (dilution: 1:1000; A1731; ABclonal) at 4°C in a humid chamber for 12–14 h. Sections were then incubated with fluorophore-conjugated anti-rabbit secondary antibody (DAKO, Santa Clara, USA) at room temperature for one hour, washed thrice with 0.1 M TBS, and mounted with DPX mounting medium. The sections were observed under a compound microscope, using appropriate filter sets[70].

4.13 Haematoxylin and Eosin (H&E) Staining

The slides were placed in a staining jar and deparaffinized by submerging them into three series of absolute xylene for 4 minutes, followed by 100%, 100%, 95%, 90%, and 70% of ethanol for 4 minutes of each percentage. The slides were thereafter washed in running tap water for 2 minutes. Then, slides were submerged into Harris Hematoxylin (Sigma-Aldrich, GERMANY) for 2 minutes and then washed in running tap water for 2 minutes, and finally mounted with a coverslip using DPX mounting after dehydration in graded ethanol. The explant tissue sections were stained with hematoxylin, and eosin for the study of Placental villi, syncytial knot formation, and stromal pathology.

4.14 Collagen Special Stain (Modified Masson's Trichrome Staining)

The early explant tissue slides were placed in a staining jar and deparaffinized by submerging into three series of absolute xylene for 4 minutes each, followed by 100%, 95%, 90%, 80%, and 70% of ethanol for 4 minutes in each percentage. The slides were then submerged in a warmed Bouin's solution at 60°C for 45 minutes. Next, the slides were washed thoroughly in running tap water until the yellow color in the samples disappeared. To differentiate nuclei, slides were

then immersed in modified Weigert's hematoxylin for 8 minutes and then washed in running water for 2 minutes. In order to stain cytoplasms and erythrocytes, slides were submerged in anionic dyes and acid fuschin (C.I. 42590, Merck, Germany) for 5 minutes; then again, slides were washed with running tap water for 2 minutes. Next, slides were treated with the phosphomolybdic acid solution for another 10 minutes as a mordant, and immediately slides were submerged into methyl blue (C.I. 42780, Merck, Germany) solution for 5 minutes in order to stain collagen and the fibroblasts. Thereafter, slides were thoroughly washed in running water for 2 minutes and lastly treated with 1% acetic acid solution for 1 minute. Slides then were dehydrated into a series of alcohol of 70%, 80%, 95%, and 100% for 1 minute for each percentage. Before observation, slides were dipped into absolute xylene for 1 minute and finally mounted with a coverslip using DPX mounting microscope (TI-E, 601869, Nikon Laser Scanning Confocal Microscope) at 200X magnification.

4.13 Statistical analysis

All experiments were repeated at least three times. Data were presented as mean ± S.D. The statistical significance of the results was assessed by Student's t-test using the Graphpad Prism software package (version 5.0; La Jolla, California, USA), with a P value less than 0.05 being considered significant.

5. Conclusion

Monosodium glutamate used as a food additive seems to affect the trophoblast function through a ROS-mediated cellular stress pathway. We presented evidence to show that trophoblast invasion and differentiation pathways are perturbed. It is, therefore, conceivable that long-term exposure to MSG might have a detrimental effect on pregnancy outcomes as represented in the graphical abstract. (Fig. 9) . Though we performed both cell line-based in-vitro as well as placental explants-based ex-vivo studies, still the lacuna of our work is to investigate the *in-vivo* effect of MSG on embryogenesis using animal models. Our study is the first report as proof of principle establishing the harmful effect of MSG on placenta and trophoblast cells. Rodent studies are currently ongoing to explore the long-term effect of MSG through the oral route on pregnancy outcome, placental function, and possibly post-natal life. Our findings are novel as, to the best of our knowledge, the effect of MSG exposure on the placenta is not addressed. Identifying its possible harmful effect on trophoblast cells will let to consume it with caution, more during pregnancy at the early stages of development.

Declarations

Data Availability:

This article contains supporting information which includes Supplementary Methods, Tables, Figures, and their Legends, and is available on the website. All the raw data of the gels and blots are available in the supplementary files. Correspondence and requests for materials should be addressed to SK (subhradip.k@aiims.edu) or RD (rubydhar@gmail.com)

Acknowledgments:

The authors are thankful to their lab technicians Mr. Vivek Raj and Mr. Dheeraj Bisht for helping them with the collection of patient samples for the study.

Author contributions:

SK, RD, and IM conceptualized the research proposal. IM conducted all the experiments with assistance from SS. SS, SG, and SB assisted in preparing the bibliography and critical discussion. TCN and IM conducted electron microscopic studies and data analysis. JBS and SK2(Supriya Kumari) helped in sample collection and discussion of clinical data. ARM and JT helped in performing the histopathological experiments. MSA and MA for their valuable suggestions and inputs related to experimental design and planning. SS, IM, and RD analyzed data and prepared illustrations. SK and IM prepared the manuscript. SK and RD planned and oversaw the entire work.

Funding and additional information:

The authors are thankful to the Indian Council of Medical Research, India for financial assistance (5/10/FR/8/2018-RBMCH to SK). IM acknowledges the Council of Scientific and Industrial Research, India for providing a Senior Research Fellowship (09/006(0495)/2019-EMR-I). The authors are grateful to the Department of Obs. & Gynae, AIIMS for providing the placental samples. The authors are grateful to the Department of Biochemistry, AIIMS, New Delhi, and Amity Institute of Biotechnology, Noida for providing support with infrastructure and logistics. MSA and MA extend their appreciation to the Deanship of Scientific Research at King Khalid University (KKU) for funding this work through the Research Group Program Under Grant Number:(R.G.P.1/256/43).

Conflict of interest:

The authors declare that they have no conflict of interest with the contents of this article.

Abbreviations

MSG, Monosodium glutamate; PE, Preeclampsia PE; ROS, Reactive oxygen species; OS, Oxidative stress; CAGR, Compound Annual Growth Rate; CNS, Central Nervous System; WST-1, water-soluble tetrazolium-1; SYN-1, Syncytin-1; SYN-2, Syncytin-2; and GCM1, Glial Cells Missing-1; DYSF, Dysferlin; β-hCG, β subunit of human chorionic gonadotropin; FT, First trimester; MTP, Medically terminated pregnancy; SLC1A5, Solute Carrier Family 1 Member 5; MFSD2A, Major Facilitator Superfamily Domain Containing 2A; EVT, Extravillous trophoblast; MMP-2, Matrix metalloproteinase-2; MMP-9, Matrix metalloproteinase- 9; TIMP-1, Tissue inhibitor of metalloproteinase-1; TIMP-2, Tissue inhibitor of metalloproteinase-2; PAI-1, plasminogen activator inhibitor-1; uPA, urokinase plasminogen activator; PLAC8, Placenta associated 8; RT-PCR, Real time PCR; NAC, N-Acetyl cysteine; TBARS, Thiobarbituric acid reactive substances; NRF2, nuclear factor erythroid 2–related factor 2; TEM, Transmission Electron Microscopy; ER, Endoplasmic reticulum; BiP, Binding immunoglobulin protein; p-IRE1a, phosphorylated inositol-requiring enzyme 1a; IRE1a, inositol-requiring enzyme 1a; Xbp1, X-box binding protein 1; IL-6,interleukin-6; TNF-a, tumor necrosis factor-alpha; miRNA, micro-RNA; DNA, Deoxyribonucleated acid; SRC, JNK , c-Jun N-terminal kinase; PKC, protein kinase C; HIF, hypoxia inducible factor; ATCC, American Type Culture Collection; PBS, phosphate-buffered saline; CO 2 , carbon dioxide; PI, propidium iodide; FITC, Fluorescein isothiocyanate; MDA, Malondialdehyde; RIPA, Radioimmunoprecipitation assay buffer; PVDF, polyvinylidene difluoride; ECL, enhanced chemiluminescence; SDS-PAGE, Sodium dodecyl sulphate-polyacrylamide gel electrophoresis; HRP, Horseradish Peroxidase; TBST, Tris buffered saline Tween; BSA, bovine serum albumin; GAPDH, glyceraldehyde-3-phosphate dehydrogenase; NaCl, Sodium chloride; Cacl 2 , calcium chloride; DAPI, 4',6-Diamidine-2'-phenylindole dihydrochloride; H 2 O 2, hydrogen peroxide; EDTA, Ethylenediamine tetraacetic acid; DPX, Dibutylphthalate Polystyrene Xylene; H&E, Haematoxylin and Eosin

References

1. Glutamic Acid and Monosodium Glutamate (MSG) Market Size is likely to reach more than 4 million tons by 2023 | Global Market Insights. https://www.mynewsdesk.com/us/global-market-insights/pressreleases/glutamic-acid-and-monosodium-glutamate-msg-market-size-is-likely-to-reach-more-than-4-million-tons-by-2023-1379400.

2. China drives MSG growth both domestically and in exports. https://www.foodnavigator-asia.com/Article/2015/10/08/China-drives-MSG-growth-both-domestically-and-in-exports.

3. Global Demand for Flavor Enhancer MSG Grows as Incomes Expand, Cultures Shift, IHS Says | Business Wire. https://www.businesswire.com/news/home/20151006005707/en/Global-Demand-for-Flavor-Enhancer-MSG-Grows-as-Incomes-Expand-Cultures-Shift-IHS-Says.

4. Ingestion of monosodium glutamate (MSG) in adult male rats reduces sperm count, testosterone, and disrupts testicular histology. https://escholarship.org/uc/item/6wq9p6zn.

5. Zanfirescu, A. *et al.* A review of the alleged health hazards of monosodium glutamate. *Compr. Rev. food Sci. food Saf.* **18**, 1111 (2019).

6. Ahluwalia, P., Tewari, K. & Choudhary, P. Studies on the effects of monosodium glutamate (MSG) on oxidative stress in erythrocytes of adult male mice. *Toxicol. Lett.* **84**, 161–165 (1996).

7. Okwudiri Onyema, O., Sylvanus Alisi, C., Oscar Okwudiri, O., Chinwe Sylvanus, A. & Adaeze Peace, I. Monosodium glutamate induces oxidative stress and affect glucose metabolism in the kidney of rats Singeing of Cattle Hides View project Monosodium Glutamate Induces Oxidative Stress and Affects Glucose Metabolism in the Kidney of Rats. *Res. Artic. Int. J. Biochem. Res. Rev.* **2**, 1–11 (2012).

8. Mondal, M., Sarkar, K., Nath, P. P. & Paul, G. Monosodium glutamate suppresses the female reproductive function by impairing the functions of ovary and uterus in rat. *Environ. Toxicol.* **33**, 198–208 (2018).

9. Mustafa, Z., Ashraf, S., Tauheed, S. F. & Ali, S. Monosodium Glutamate, Commercial Production, Positive and Negative Effects on Human Body and Remedies - A Review. *undefined* (2017) doi:10.32628/IJSRST173490.

10. Hernández-Bautista, R. J. *et al.* Biochemical Alterations during the Obese-Aging Process in Female and Male Monosodium Glutamate (MSG)-Treated Mice. *Int. J. Mol. Sci.* **15**, 11473 (2014).

11. María Catalina, O. *et al.* Monosodium Glutamate Affects Metabolic Syndrome Risk Factors on Obese Adult Rats: A Preliminary Study. *J. Obes. Weight. Medicat.* **4**, (2018).

12. Hajihasani, M. M., Soheili, V., Zirak, M. R., Sahebkar, A. & Shakeri, A. Natural products as safeguards against monosodium glutamate-induced toxicity. *Iran. J. Basic Med. Sci.* **23**, 416 (2020).

13. Kazmi, Z., Fatima, I., Perveen, S. & Malik, S. S. Monosodium glutamate: Review on clinical reports. *Int. J. Food Prop.* **20**, 1807–1815 (2017).

14. Niaz, K., Zaplatic, E. & Spoor, J. Extensive use of monosodium glutamate: A threat to public health? *EXCLI J.* **17**, 273 (2018).

15. Lucas, D. R. & Newhouse, J. P. The toxic effect of sodium L-glutamate on the inner layers of the retina. *AMA. Arch. Ophthalmol.* **58**, 193–201 (1957).

16. Hossain, A., Roy, S. & Datta, A. An Overview on Monosodium Glutamate: Its direct and indirect effects 'Measurement of solubility and solvation thermodynamics of pharmaceutically important biomolecules in mixed solvent systems by experimental and theoretical modeling' View project NSOU RESEARCH GRANT View project Arup Datta Shibpur dinobundhoo Institution An Overview on Monosodium Glutamate: Its direct and indirect effects. *Artic. Res. J. Pharm. Technol.* **12**, (2019).

17. Manal Said, T. & Nawal, A.-B. Adverse Effects of Monosodium Glutamate on Liver and Kidney Functions in Adult Rats and Potential Protective Effect of Vitamins C and E. *Food Nutr. Sci.* **2012**, 651–659 (2012).

18. Bhattacharya, T., Bhakta, A. & Ghosh, S. K. Long term effect of monosodium glutamate in liver of albino mice after neo-natal exposure.

19. Egbuonu, A. C. C., Obidoa, O., Ezeokonkwo, C. A., Ezeanyika, L. U. S. & Ejikeme, P. M. Hepatotoxic effects of low dose oral administration of monosodium glutamate in male albino rats. *African J. Biotechnol.* **8**, 3031–3035 (2009).

20. Ali, A. A., El-Seify, G. H., Haroun, H. M. El & Soliman, M. A. E. M. M. Effect of monosodium glutamate on the ovaries of adult female albino rats and the possible protective role of green tea. *Menoufia Med. J.* **27**, 793 (2014).

21. Eweka, A. & Om'Iniabohs, F. Histological Studies of the Effects of Monosodium Glutamate on the Ovaries of Adult Wistar Rats. *Ann. Med. Health Sci. Res.* **1**, 37 (2011).

22. (PDF) Effects of Monosodium Glutamate in Ovaries of Female Sprague-Dawley Rats. https://www.researchgate.net/publication/284730349_Effects_of_Monosodium_Glutamate_in_Ovaries_of_Female_Sprague-Dawley_Rats.

23. Ajani, E., Ogunlabi, O., Adegbesan, B., Adeosun, O. & Akinwande, O. Nigerian mistletoe (*Loranthus micranthus*Linn) aqueous leaves extract modulates some cardiovascular disease risk factors in monosodium glutamate induced metabolic dysfunction. *African J. Biotechnol.* **13**, (2015).

24. Hazzaa, S. M., El-Roghy, E. S., Abd Eldaim, M. A. & Elgarawany, G. E. Monosodium glutamate induces cardiac toxicity via oxidative stress, fibrosis, and P53 proapoptotic protein expression in rats. *Environ. Sci. Pollut. Res. 2020 2716* **27**, 20014–20024 (2020).

25. Monosodium glutamate is related to a higher increase in bloo... : Journal of Hypertension. https://journals.lww.com/jhypertension/Fulltext/2011/05000/Monosodium_glutamate_is_related_to_a_higher.7.aspx?casa_token=aJdbM7DtJLIAAAAA:jUcuUMa7zbfVO3z5pePSmEK0KDhinVU9w70RlFtabjzSElnNQgxMC9DX7qLCscthY3uF0RxsHuzfgMKvRcDthqzFVbA4iN21E(

26. Chakraborty, S. P. Patho-physiological and toxicological aspects of monosodium glutamate. *https://doi.org/10.1080/15376516.2018.1528649* **29**, 389–396 (2019).

27. Lopes, F. N. C. *et al.* Antioxidant therapy reverses sympathetic dysfunction, oxidative stress, and hypertension in male hyperadipose rats. *Life Sci.* **295**, 120405 (2022).

28. Dhar, R. *et al.* MTiness in pseudo-malignant behavior of trophoblasts during embryo implantation. *Front. Biosci. - Landmark* **26**, 717–743 (2021).

29. Cohen, M. & Bischof, P. Factors Regulating Trophoblast Invasion. *Gynecol. Obstet. Invest.* **64**, 126–130 (2007).

30. Chang, W. L. *et al.* Plac8, a new marker for human interstitial extravillous trophoblast cells, promotes their invasion and migration. *Dev.* **145**, (2018).

31. Farombi, E. O. & Onyema, O. O. Monosodium glutamate-induced oxidative damage and genotoxicity in the rat: Modulatory role of vitamin C, vitamin E and quercetin. *Hum. Exp. Toxicol.* **25**, 251–259 (2006).

32. (PDF) Monosodium glutamate induces oxidative stress and affect glucose metabolism in the kidney of rats. https://www.researchgate.net/publication/298105979_Monosodium_glutamate_induces_oxidative_stress_and_affect_glucose_metabolism_in_the_kidney_of_r

33. MSG—monosodium glutamate - Cancer FactFinder. https://cancerfactfinder.org/diet-nutrition/monosodium-glutamate/.

34. Al-Agili, Z. H. The Effect of Food Additives (Monosodium Glutamate - MSG) On Human Health - A Critical Review. *J. AlMaarif Univ. Coll.* 362–369 (2020) doi:10.51345/.V31I1.235.G162.

35. Das, D., Banerjee, A., Bhattacharjee, A., Mukherjee, S. & Maji, B. K. Dietary food additive monosodium glutamate with or without high-lipid diet induces spleen anomaly: A mechanistic approach on rat model. *Open Life Sci.* **17**, 22 (2022).

36. Araujo, T. R. *et al.* Benefits of l-alanine or l-arginine supplementation against adiposity and glucose intolerance in monosodium glutamate-induced obesity. *Eur. J. Nutr.* **56**, 2069–2080 (2017).

37. He, K. *et al.* Consumption of monosodium glutamate in relation to incidence of overweight in Chinese adults: China Health and Nutrition Survey (CHNS). *Am. J. Clin. Nutr.* **93**, 1328–1336 (2011).

38. Collison, K. S. *et al.* Interactive effects of neonatal exposure to monosodium glutamate and aspartame on glucose homeostasis. *Nutr. Metab.* **9**, 1–13 (2012).

39. Rahayu, M. S., Sri Wahyuni & Yuziani. Effects of Oral Administration of Monosodium Glutamate (MSG) on Obesity in Male Wistar Rats (Rattus Norvegicus). *Biosci. Med. J. Biomed. Transl. Res.* **5**, 879–882 (2021).

40. Roman-Ramos, R. *et al.* Monosodium glutamate neonatal intoxication associated with obesity in adult stage is characterized by chronic inflammation and increased mRNA expression of peroxisome proliferator-activated receptors in mice. *Basic Clin. Pharmacol. Toxicol.* **108**, 406–413 (2011).

41. Long term effects of monosodium glutamate on spermatogenesis following neonatal exposure in albino mice–a histological study | Request PDF. https://www.researchgate.net/publication/50905995_Long_term_effects_of_monosodium_glutamate_on_spermatogenesis_following_neonatal_exposure_in_a-a_histological_study.

42. Merve Bayram, H., Fatih Akgoz, H., Kizildemir, O. & Ozturkcan, A. Monosodium Glutamate: Review on Preclinical and Clinical Reports. **13**, 149 (2023).

43. Monosodium Glutamate, Commercial Production, Positive and Negative Effects on Human Body and Remedies - A Review | Semantic Scholar. https://www.semanticscholar.org/paper/Monosodium-Glutamate%2C-Commercial-Production%2C-and-on-Mustafa-Ashraf/391860fc838ab808c7ca4ebd079bf80bf439119f.

44. Airaodion, A. I. Toxicological Effect of Monosodium Glutamate in Seasonings on Human Health. *Glob. J. Nutr. Food Sci.* **1**, (2019).

45. Harvest of the Sea Launches Seafood Medley at Costco Locations Regionally | News | wfmz.com. https://www.wfmz.com/news/pr_newswire/pr_newswire_food_beverages/harvest-of-the-sea-launches-seafood-medley-at-costco-locations-regionally/article_5698eb68-5b02-5786-a896-844347a68d85.html.

46. Monosodium Glutamate (MSG) - Chemical Economics Handbook (CEH) | IHS Markit. https://ihsmarkit.com/products/monosodium-glutamate-chemical-economics-handbook.html.

47. Banerjee, A., Mukherjee, S. & Maji, B. K. Worldwide flavor enhancer monosodium glutamate combined with high lipid diet provokes metabolic alterations and systemic anomalies: An overview. *Toxicol. Reports* **8**, 938 (2021).

48. Pavlovic, V. *et al.* Effect of monosodium glutamate on oxidative stress and apoptosis in rat thymus. *Mol. Cell. Biochem.* **303**, 161–166 (2007).

49. Rosa, S. G., Chagas, P. M., Pesarico, A. P. & Nogueira, C. W. Monosodium glutamate induced nociception and oxidative stress dependent on time of administration, age of rats and susceptibility of spinal cord and brain regions. *Toxicol. Appl. Pharmacol.* **351**, 64–73 (2018).

50. Yang, Y. *et al.* Reactive Oxygen Species are Essential for Placental Angiogenesis During Early Gestation. *Oxid. Med. Cell. Longev.* **2022**, 1–14 (2022).

51. Weaver, A. M. Regulation of Cancer Invasion by Reactive Oxygen Species and Tks Family Scaffold Proteins. *Sci. Signal.* **2**, pe56 (2009).

52. Perillo, B. *et al.* ROS in cancer therapy: the bright side of the moon. *Exp. Mol. Med. 2020 522* **52**, 192–203 (2020).

53. Gopalakrishna, R. & Jaken, S. Protein kinase C signaling and oxidative stress. *Free Radic. Biol. Med.* **28**, 1349–1361 (2000).

54. Lyall, F. The human placental bed revisited. *Placenta* **23**, 555–562 (2002).

55. Foidart, J. M., Hustin, J., Dubois, M. & Schaaps, J. P. The human placenta becomes haemochorial at the 13th week of pregnancy. *Int. J. Dev. Biol.* **36**, 451–453 (2002).

56. Ahmed, A., Dunk, C., Ahmad, S. & Khaliq, A. Regulation of placental vascular endothelial growth factor (VEGF) and placenta growth factor (PIGF) and soluble Flt-1 by oxygen - A review. *Placenta* **21**, (2000).

57. Forsythe, J. A. *et al.* Activation of vascular endothelial growth factor gene transcription by hypoxia-inducible factor 1. *Mol. Cell. Biol.* **16**, 4604–4613 (1996).

58. Jauniaux, E., Hempstock, J., Greenwold, N. & Burton, G. J. Trophoblastic oxidative stress in relation to temporal and regional differences in maternal placental blood flow in normal and abnormal early pregnancies. *Am. J. Pathol.* **162**, 115–125 (2003).

59. Jauniaux, E., Greenwold, N., Hempstock, J. & Burton, G. J. Comparison of ultrasonographic and Doppler mapping of the intervillous circulation in normal and abnormal early pregnancies. *Fertil. Steril.* **79**, 100–106 (2003).

60. Huppertz, B. The Critical Role of Abnormal Trophoblast Development in the Etiology of Preeclampsia. *Curr. Pharm. Biotechnol.* **19**, 771–780 (2018).

61. Weiss, G., Sundl, M., Glasner, A., Huppertz, B. & Moser, G. The trophoblast plug during early pregnancy: a deeper insight. *Histochem. Cell Biol.* **146**, 749–756 (2016).

62. Mukherjee, I. *et al.* Oxidative stress-induced impairment of trophoblast function causes preeclampsia through the unfolded protein response pathway. *Sci. Rep.* **11**, (2021).

63. Xu, X. *et al.* Retraction for Xu et al., Reactive oxygen species-triggered trophoblast apoptosis is initiated by endoplasmic reticulum stress via activation of caspase-12, CHOP, and the JNK pathway in Toxoplasma gondii infection in mice. *Infect. Immun.* **83**, 1735 (2015).

64. Fisher, J. J., Bartho, L. A., Perkins, A. V. & Holland, O. J. Placental mitochondria and reactive oxygen species in the physiology and pathophysiology of pregnancy. *Clin. Exp. Pharmacol. Physiol.* **47**, 176–184 (2020).

65. Greenbaum, S. *et al.* Spatio-temporal coordination at the maternal-fetal interface promotes trophoblast invasion and vascular remodeling in the first half of human pregnancy. *bioRxiv* 2021.09.08.459490 (2021).

66. Sharma, S., Godbole, G. & Modi, D. Decidual Control of Trophoblast Invasion. *Am. J. Reprod. Immunol.* **75**, 341–350 (2016).

67. Ma, Q. Role of Nrf2 in Oxidative Stress and Toxicity. *Annu. Rev. Pharmacol. Toxicol.* **53**, 401 (2013).

68. Tebay, L. E. *et al.* Mechanisms of activation of the transcription factor Nrf2 by redox stressors, nutrient cues, and energy status and the pathways through which it attenuates degenerative disease. *Free Radic. Biol. Med.* **88**, 108 (2015).

69. Kobayashi, M. *et al.* The Antioxidant Defense System Keap1-Nrf2 Comprises a Multiple Sensing Mechanism for Responding to a Wide Range of Chemical Compounds. *Mol. Cell. Biol.* **29**, 493–502 (2009).

70. Mukherjee, I. *et al.* Oxidative stress-induced impairment of trophoblast function causes preeclampsia through the unfolded protein response pathway. *Sci. Reports 2021 111* **11**, 1–20 (2021).

Figures

Fig 1.

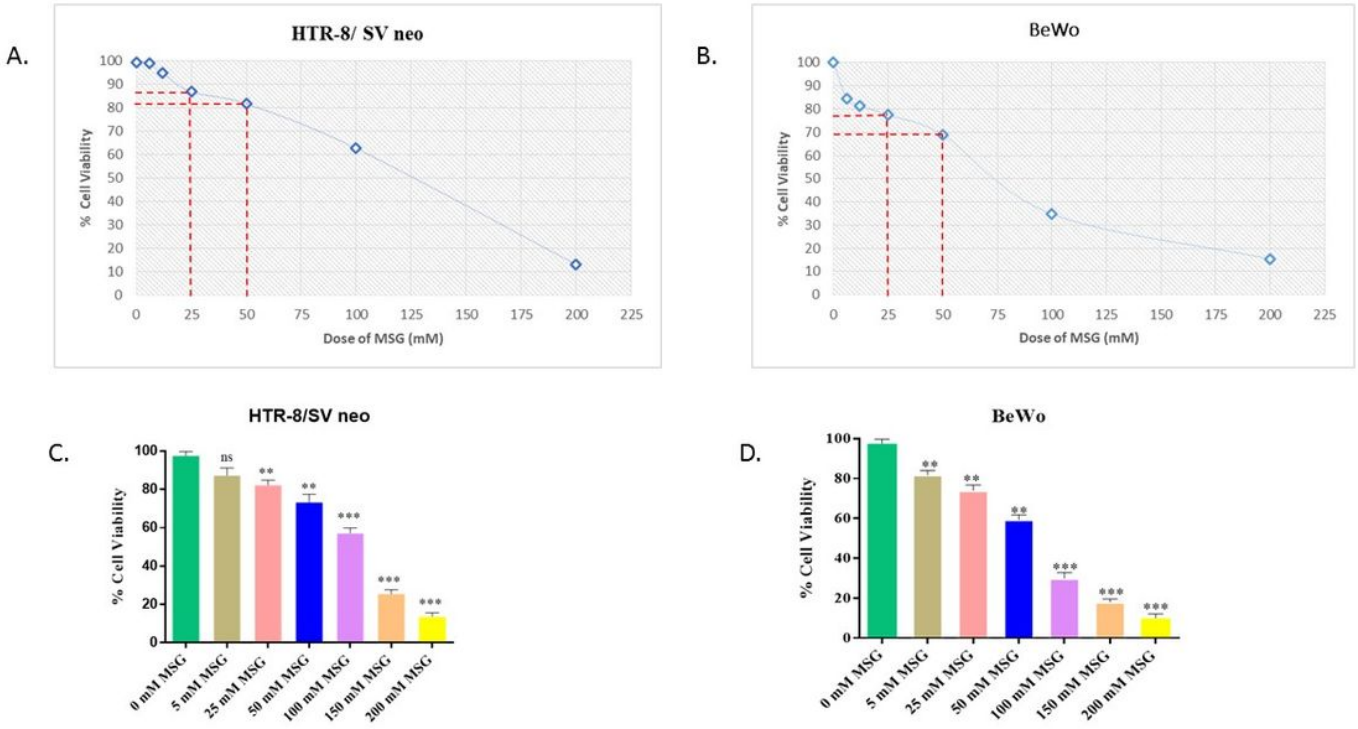

Figure 1

Effect of MSG on the viability of BeWo and HTR8/SVneo cells. (A-B) WST-1 assay and Trypan Blue staining were done to assess and quantify the viability of cells. Cells were treated with different doses of MSG to check their viability (expressed as percentage viability) . WST-1 assay was performed with BeWo and HTR8/SVneo cells to check the sub-lethal dose. **(C-D)** The trophoblast cells HTR8/SVneo and BeWo were also stained with trypan blue after treating them with the different doses of MSG, and the results were plotted graphically. Results are representative of at least three independent experiments

Fig 2.

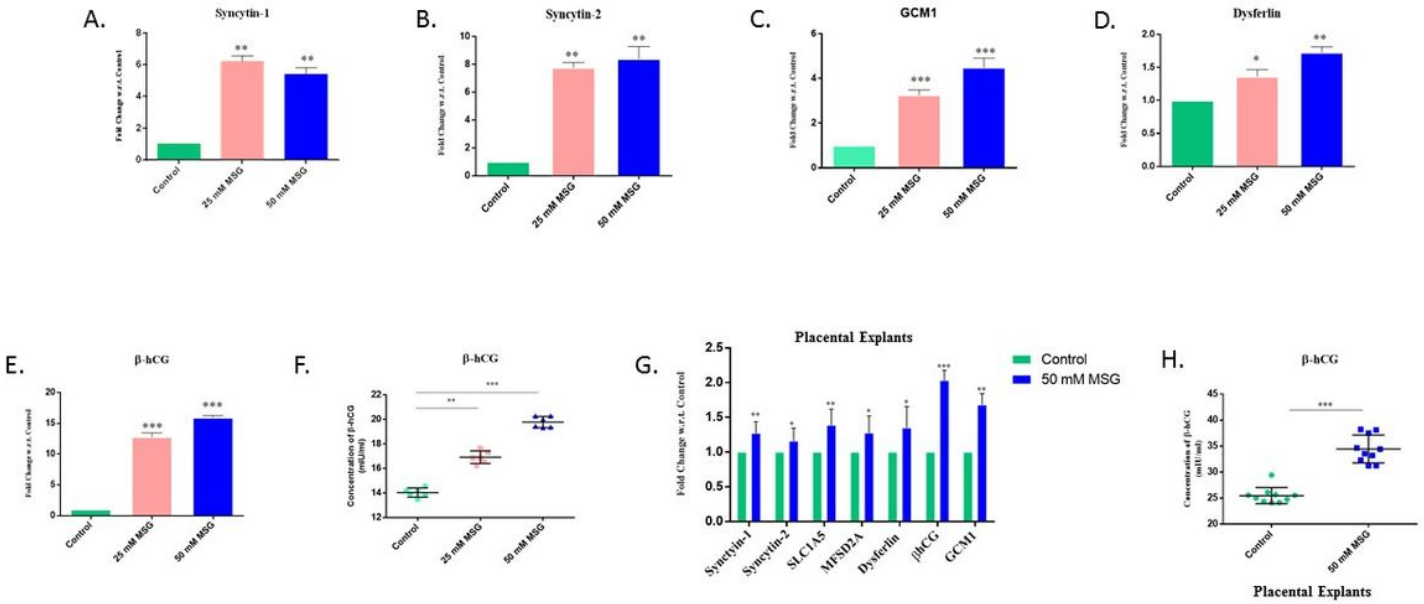

Figure 2

Expression of differentiation markers after short term(acute) stimulation of MSG in the trophoblast cells and placental explant tissues. (A-E). qPCR showing fold change in the mRNA expression of differentiation markers in the BeWo cells after acute stimulation of MSG (25mM and 50 mM) for 24h. The results were analyzed by the $2^{-\triangle C.T}$. method (△C.T. = C.T. value of sample -C.T. value of internal reference gene). **(F)** Quantification of β-hCG in the conditioned media of the treated early placental explants using ELISA assay. **(G)** qPCR showing fold change in the mRNA expression of differentiation markers in the tissue explants from early placentas treated with 50 mM MSG **(H)** Quantification of β-hCG in the conditioned media of the treated early placental explants using ELISA assay. (n=10). All data are represented as Mean ± Standard deviation. Results are representative of at least three independent experiments. * $p < 0.05$; ** $p < 0.01$; *** $p < 0.001$.

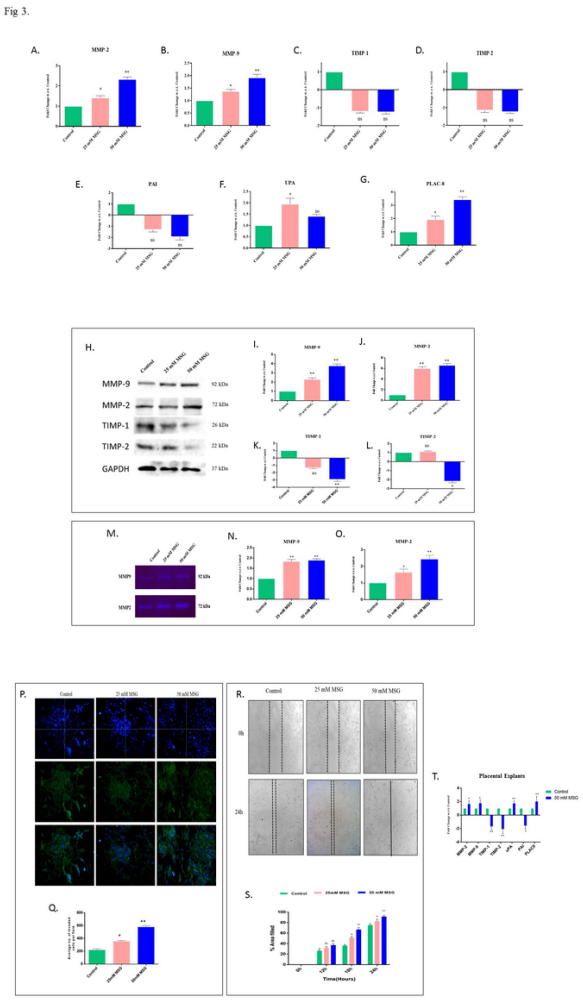

Figure 3

MSG alters the level of protease and their inhibitors (A-G). qPCR was performed to quantify the change in mRNA expression MMP-2, MMP-9, TIMP-1, TIMP-2, UPA, PAI, and PLAC8, in the untreated and treated HTR8/SVneo trophoblast cells. Statistical analysis was done by comparing the fold change in the 25mM and 50 mM MSG treated group with respect to the Control. The results were analyzed by the 2−△△C.T. method (△△C.T. = △C.T. value of Treatment -△C.T. value of another treatment. **(H)** Western blot shows the protein levels of MMPs and their inhibitors. GAPDH served as the loading control. **(I-L)** Band intensities were measured, and normalization was done using GAPDH values. Band intensities were quantified using ImageJ and plotted graphically. Original blots are presented in Suppl Fig.4(A-E). **(M-O)** Gelatin Zymography was performed with the cell-supernatant from MSG stimulated cells and Control to assess the activity of MMP-2 and MMP-9. Quantification of the band intensities was performed using ImageJ software and plotted graphically. Original gels are presented in Suppl Fig.5. **(P-Q)** Matrigel invasion assay was done to assess the effect of monosodium glutamate on the invasiness of HTR8/SVneo trophoblast cells (n=3). The images of invaded cells were taken by using a fluorescence microscope by staining with Phalloidin and DAPI. The result was measured by counting the average number of invaded cells in four random fields using ImageJ, and data were plotted graphically. **(R-S)** Wound healing assay was performed to assess the effect of short term stimulation of MSG on the migratory behavior of the trophoblast cells. Evenly distributed scratches were made, and the healing of the scratch was observed for 24 hours. The wound area was calculated using ImageJ for every designated time interval. Fold difference in the extent of the area filled was calculated and plotted graphically for each time interval. **(T)** mRNA expression MMP-2, MMP-9, TIMP-1, TIMP-2, UPA, PAI, and PLAC8, in the early placental explants (n=10) treated with 50 mM MSG was checked. All data in the figure are shown as Mean ± Standard deviation. Results are representative of at least three independent experiments. * $p < 0.05$; ** $p < 0.01$; *** $p < 0.001$.

Fig 4.

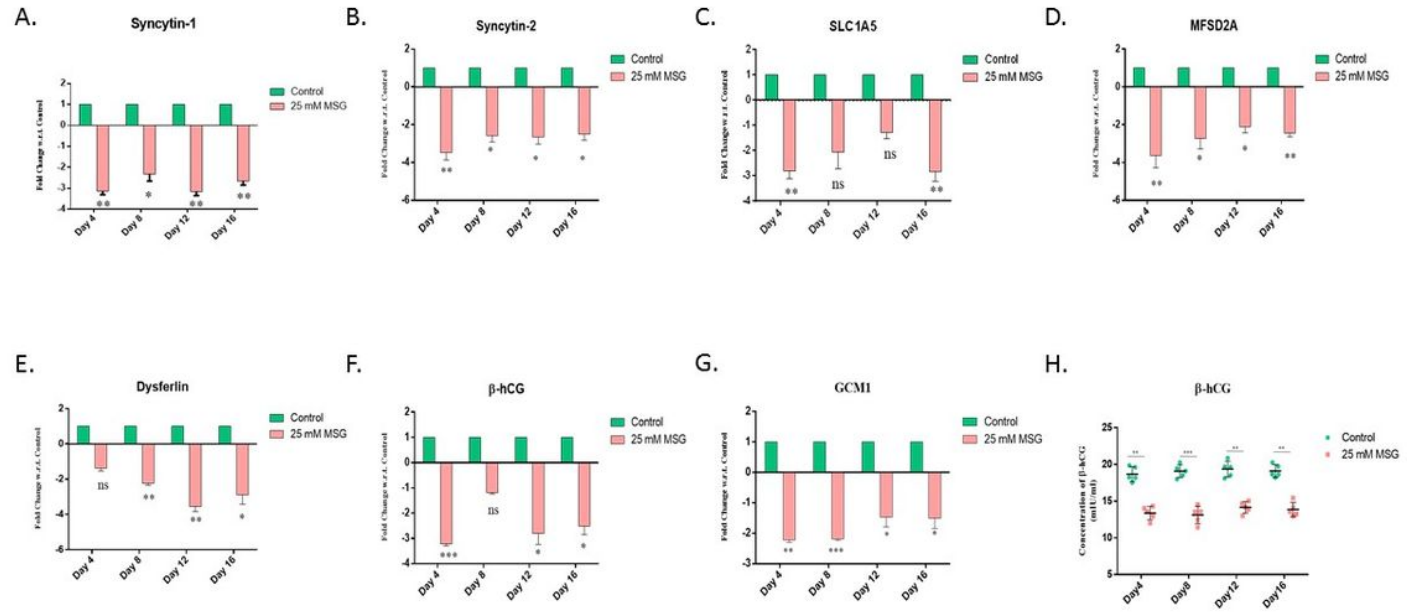

Figure 4

Expression of differentiation markers decreases after chronic stimulation of MSG in the BeWo cells. (A-G). qPCR showing fold change in the mRNA expression of differentiation markers in the BeWo cells after chronic stimulation of MSG (25mM) for 16 consecutive days. The data points were taken on days 4, 8, 12, and 16. The results were analyzed by the $2^{-\triangle C.T}$. method (△C.T. = C.T. value of sample -C.T. value of internal reference gene). **(G)** Quantification of β-hCG in the conditioned media of the treated cells using ELISA assay. All data are shown as Mean ± Standard deviation. Results are representative of at least three independent experiments. * $p < 0.05$; ** $p < 0.01$; *** $p < 0.001$.

Fig 5.

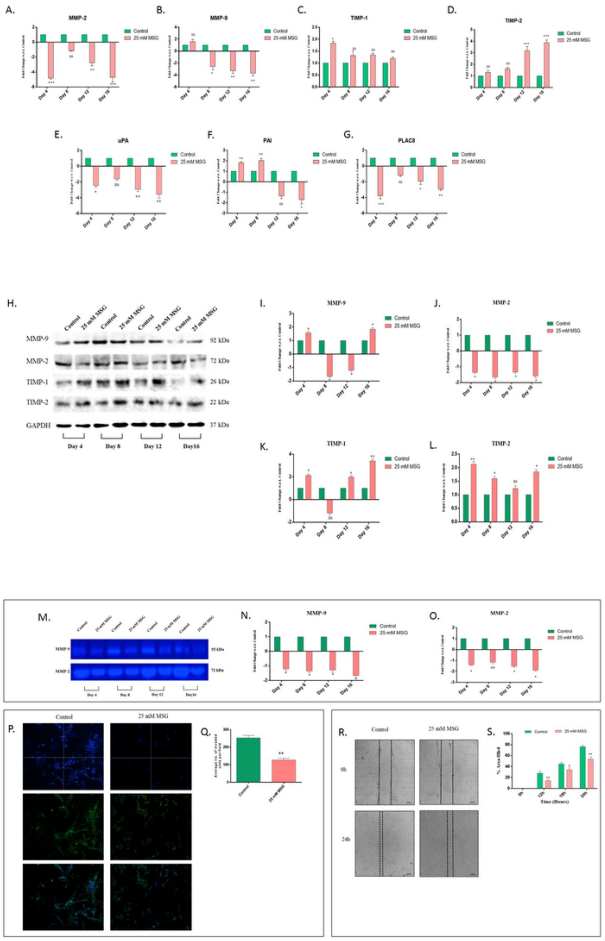

Figure 5

Chronic stimulation of MSG in the HTR-8/SV neo cells decreases their invasive and migratory property. (A-G) qPCR was performed to quantify the change in mRNA expression MMP-2, MMP-9, TIMP-1, TIMP-2, UPA, PAI, and PLAC8, in the HTR8/SVneo trophoblast cells treated with 25 mM MSG for a continuous span of 16 days. Statistical analysis was done by comparing the fold change in the 25mM and 50 mM MSG treated group with respect to the Control. The results were analyzed by the $2^{-\triangle\triangle}$C.T. method ($\triangle\triangle$C.T. = $\triangle$C.T. value of Treatment -$\triangle$C.T. value of another treatment. **(H)** Western blotting shows the protein levels of the proteases (MMP-2, MMP-9) and their inhibitors (TIMP-1 and TIMP-2). GAPDH was taken as the loading control. **(I-L)** Band intensities were quantified and normalized over the GAPDH values. Band intensities were quantified using ImageJ and plotted graphically. Original blots are presented in Suppl Fig.6(A-E). **(M-O)** Gelatin Zymography was performed with the cell supernatant from stimulated cells and Control to observe the activity of MMP-2 and MMP-9 on Day 4, Day 8, Day 12, and Day 16 of 25 mM MSG stimulation. The band intensities were quantified using ImageJ and plotted graphically. Original gels are presented in Suppl Fig.7. **(P-Q)** Matrigel invasion assay was performed to check the effect of chronic monosodium glutamate on the invasiveness of HTR8/SVneo trophoblast cells. The images obtained of the invaded cells were taken by using a fluorescence microscope by staining with Phalloidin and DAPI. The result was quantified by counting the average number of invaded cells in four random fields using ImageJ, and data were plotted graphically. **(R-S)** . Scratch Assay was done to assess the effect of acute stimulation of MSG on the migratory behavior of the trophoblast cells. Equal scratches were made in both the treated and the untreated groups, and the healing of the wound was observed for 24 hours. The wound area was calculated using ImageJ for every designated time interval. Fold difference in the extent of the area filled was calculated and plotted graphically for each time interval. All data are shown as Mean ± Standard deviation. Results are representative of at least three independent experiments. * $p < 0.05$; ** $p < 0.01$; *** $p < 0.001$.

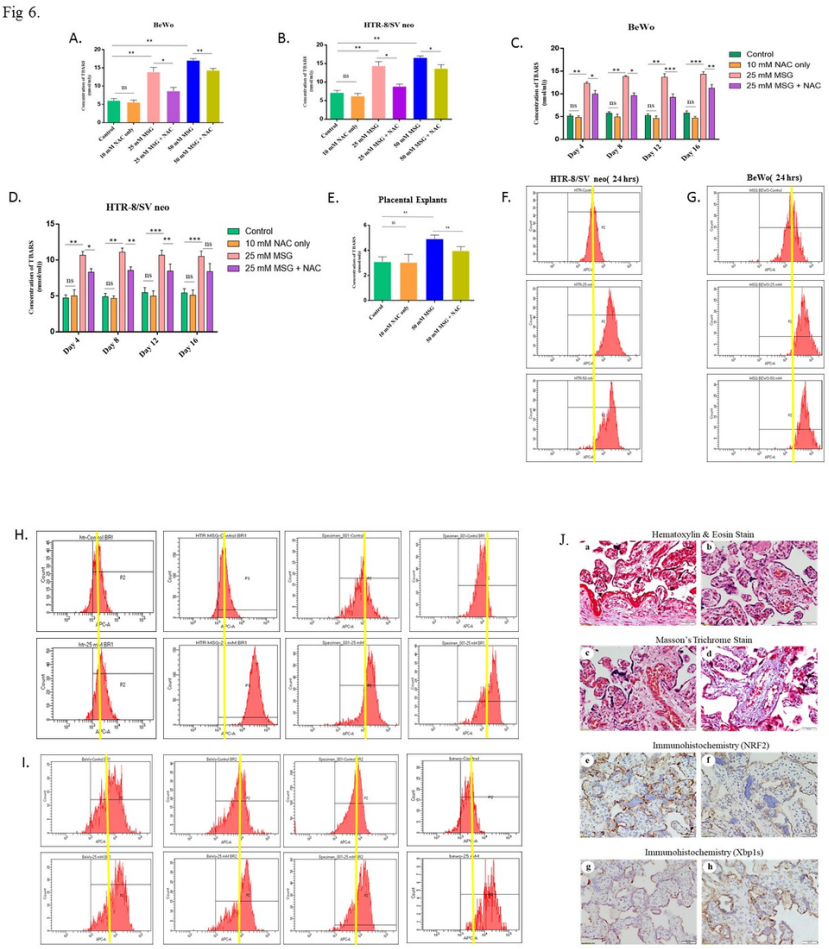

Figure 6

MSG induces ROS generation in BeWo and HTR8/SVneo cells. Lipid peroxidation product TBARS was quantified in untreated and treated BeWo **(A)** and HTR8/SVneo **(B)** to check the production of ROS in the trophoblast cells after acute stimulation of 25 mM and 50 mM MSG using ELISA. N-Acetyl Cysteine (NAC) was used as the antioxidant to quench the effects of ROS. Similarly, to check the chronic effects of MSG in the BeWo and HTR-8/SV neo trophoblast cells, ELISA was performed taking data points of Day4, Day 8, Day 12, and Day 16, and data was plotted graphically **(C-D)**. **(E)** TBARS was also measured in the conditioned media obtained from the early placental explants treated with 50 mM MSG. 10 mM NAC was used as the antioxidant in the same. ROS production was determined in the untreated and MSG stimulated HTR8/SVneo **(F)** and BeWo **(G)** trophoblast cells; n=3. Using Cell ROX Deep Red staining. Data represented a shift in peak with increased ROS production in BeWo and HTR8/SVneo cells; n=3. A false line was used to show the shift in the peaks after stimulation of MSG. ROS levels were also determined in the chronic MSG treated groups using Cell ROX Deep Red staining in both the trophoblast cells **(H-I)**. All data are shown as Mean ± Standard deviation. **(J)** Hematoxylin and Eosin . Eosin stained (HE) sections from first-trimester placenta shows well-vascularized villi and presence of syncytial knots in both (a) control and (b) treated groups. Collagenous matrix is greater as compared to (c) control in the stroma of (d) treated explant. NRF2 immunopositivity is greater in (e) control than that of (f) explant after MSG treatment. XBP1s immunopositivity is lesser in (g) control than that of (h) explant after MSG treatment. Results are representative of at least three independent experiments. * $p < 0.05$; ** $p < 0.01$; *** $p < 0.001$; **** $p < 0.0001$.

Fig 7.

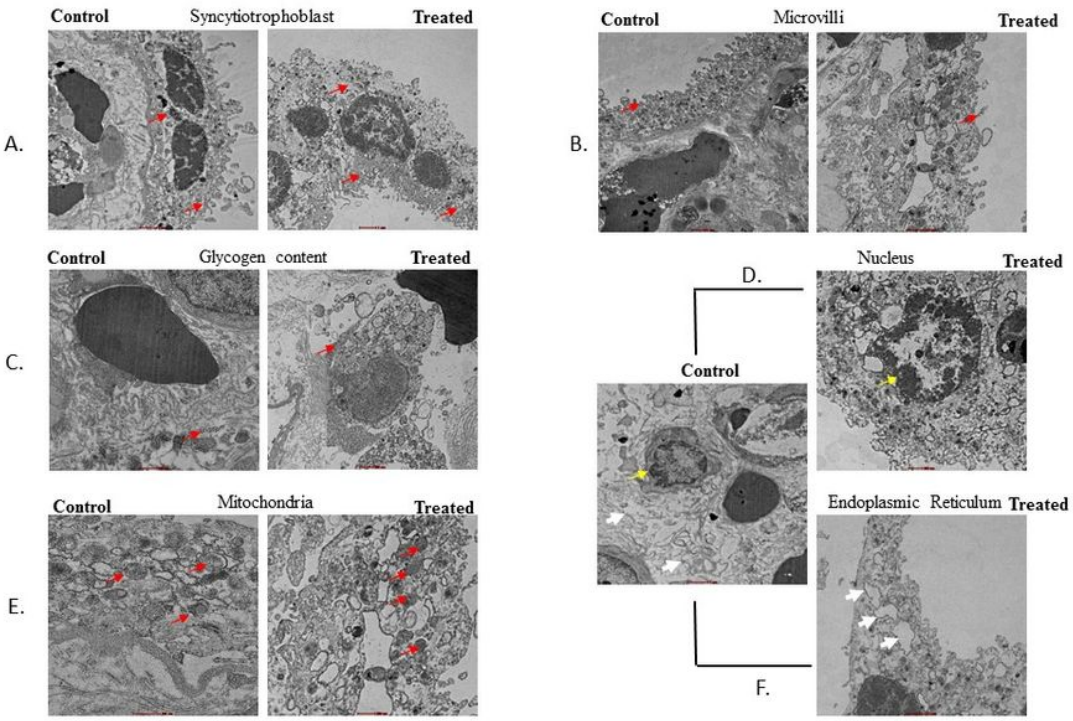

Figure 7

Ultrastructural changes in MSG treated early placental explants compared to the untreated explants. Transmission electron micrographs showing ultrastructural features in the early placental explant samples. Arrows indicate the individual parameters in each image. **(A)** Syncytiotrophoblasts (**B)** Microvilli. Microvilli were tiny, reduced, and fragmented in a number of early explant tissues. **(C)** Glycogen content was high in the MSG-treated tissues. **(D)** Nucleus. The MSG treated explants had disintegrated nucleus compared to the untreated control explants. **(E)** Mitochondrial profile. The MSG treated early explants were observed to have compromised mitochondria. **(F)** The MSG-treated tissue explants had distorted, and swollen E.R. Results are representative of at least ten independent experiments.

Fig 8.

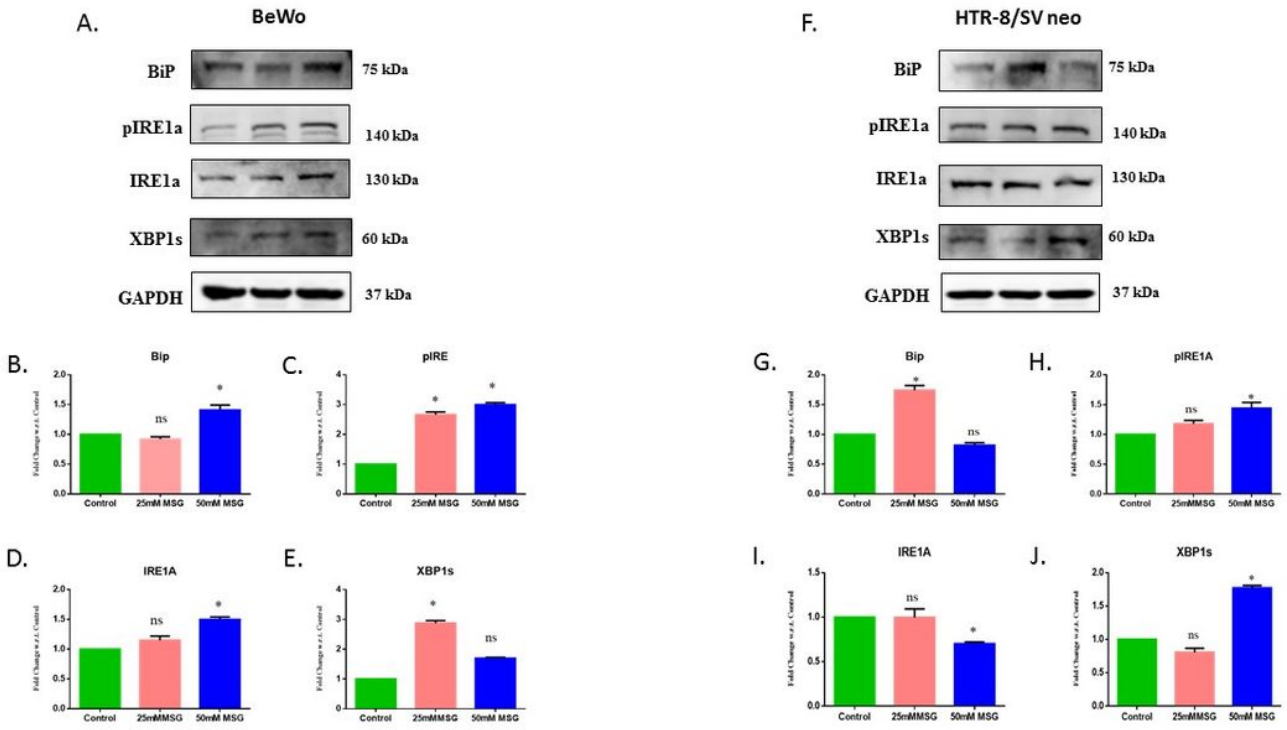

Figure 8

MSG induced E.R. stress through the UPR pathway in trophoblast cells HTR8/SVneo and BeWo. (A) Western blotting was done (n=3) to check and quantify the expression of proteins involved in the UPR pathway. Lysates isolated and prepared from the untreated and acute MSG treated. BeWo cells were immunoblotted for BiP, IRE1α, pIRE1α, and XBP-1s. GAPDH served as the loading control. Band intensities obtained were quantified and normalized over the GAPDH values, which were taken as the loading control. **(B-E)** Band intensities were measured using ImageJ and plotted graphically. **(F)** Lysates isolated and prepared from treated and untreated groups of HTR8/SVneo cells with 25 mM of MSG (n=3) were immunoblotted for BiP, IRE1α, XBP-1s in both HTR-8/SV neo and BeWo cells. GAPDH was taken as the loading control. The observed band intensities were quantified and normalized over the GAPDH values. **(G-J)** Band intensities were quantified using ImageJ and plotted graphically. Original blots are presented in Suppl Fig.8(A-F). All data obtained are shown as Mean ± Standard deviation. The results shown are representative of at least three independent experiments. * $p < 0.05$; ** $p < 0.01$; *** $p < 0.001$. **** $p < 0.0001$

Fig 9.

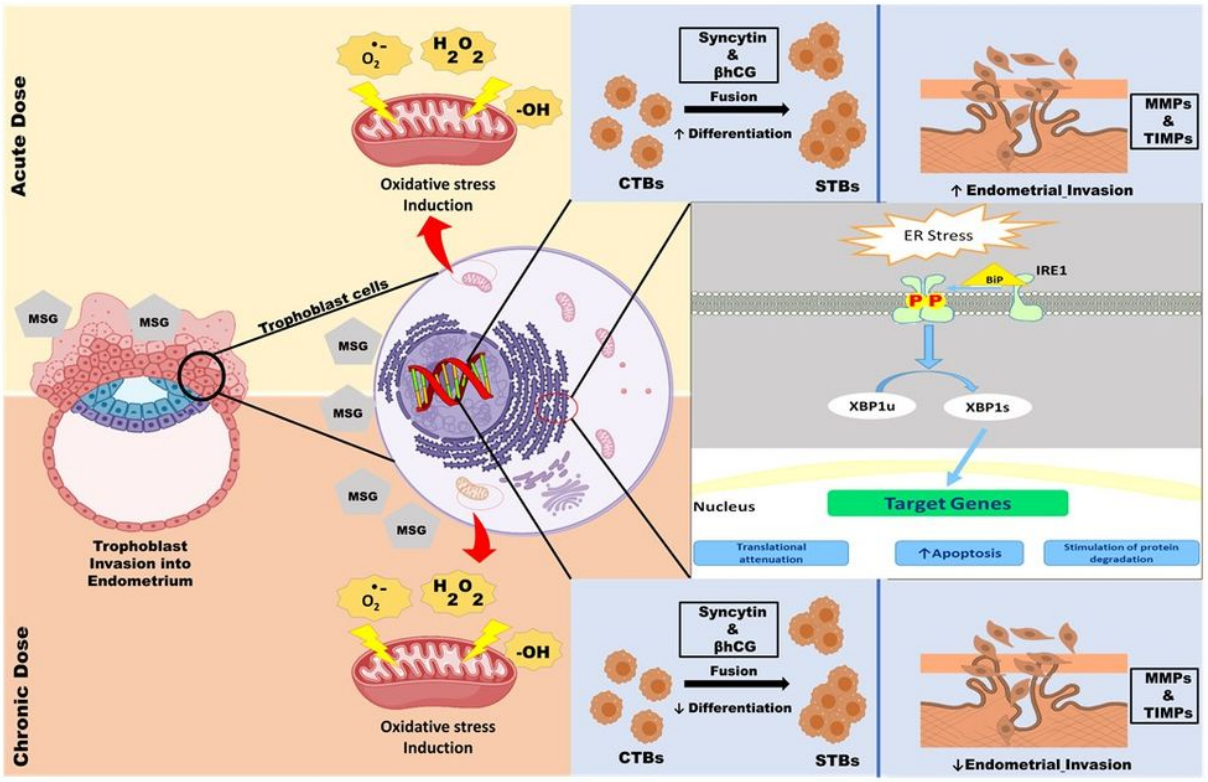

Figure 9

Graphical representation. The pictorial, abstract showing both acute and chronic monosodium glutamate-mediated alteration in the differentiation and invasion-migration behavior of the trophoblasts. MSG also induces oxidative stress in the trophoblasts, thereby leading to the endoplasmic reticulum (ER) injury and protein misfolding in the cells by engagement of unfolded protein response (UPR) pathway.

Supplementary Files

This is a list of supplementary files associated with this preprint. Click to download.

- SupplementarydetailsKarmakaretal.docx